Google Earth Engine for Monitoring Drought Impacts on Urban Tree using the Standardized Vegetation Index (SVI) in Amphoe Mueang, Nakhonratchasima Province, Thailand

Pongpun Juntakut[1], Yaowaret Jantakat[2], Chomphak Jantakat[3]

[1] *Department of Civil Engineering, Academic Division of Chulachomklao Royal Military Academy, Nakhon-Nayok 26001, Thailand*
[2] *Information and Communication of Technology, Faculty of Sciences and Liberal Arts, Rajamangala University of Technology Isan, Nakhonratchasima 30000, Thailand*
[3] *Vongchavalitkul University, Nakhonratchasima 30000, Thailand*

*Corresponding author; E-mail address: juntakut37@gmail.com or pongpun.ju@crma.ac.th
Received: 27 Jun 2021; Revised from: 19 Dec 2021; Accepted: 23 Dec 2021
Print-ISSN: 2228-9135, Electronic-ISSN: 2258-9194, doi: 10.14456/built.2021.__

Abstract

The study aimed to apply the Google Earth Engine (GEE) for monitoring drought impacts on urban tree with the Standardized Vegetation Index (SVI) for long-term and near real-time period in Amphoe Mueang, Nakhonratchasima Province, Thailand. Terra/MODIS satellites from 2000 to recently were analyzed and accessed drought impacts on urban tree in the study area. The results of this study indicated that the SVI values (-2.50 to -1.50) in the condition of very high drought were found mostly in 2019, especially in summer season and with an increasing trend of higher drought in the middle of the study area (Tambon Nai Mueang) and in the south part of the study area (Tambon Nong Chabok, Pho Klang, and Nong Bua Sala) where should be seriously realized and considered on coming dry conditions. Based on the SVI timeseries, the condition of high drought (-1.5 to -0.5) was obviously found in years of 2002, 2005, 2015, 2016, and 2019. In addition, the study demonstrated that the GEE could display the SVI image of the whole timescale in the map section and can receive a pixel value from the visualized SVI images by clicking on a location within the study area in long-term and near real-time period. Conclusively, the application of the GEE for monitoring drought impacts on urban tree can be an efficiency tool for planning urban management to mitigate the impact of drought on urban tree and is helpful to take care of tree growth in urban area.

Keywords: Google Earth Engine, Drought, Urban Tree, Standardized Vegetation Index, Terra/MODIS satellite

1. Introduction

Droughts are recognized as a complex natural phenomenon that impacts on water resources, agriculture, natural ecosystems, and society (Chen et al., 2013; Zhang et al., 2015; Wang et al., 2014; Wang and Meng, 2013). Recently, due to the change in climate, drought is expected to increase in frequency and severity. Additionally, drought impacts on urban tree and crop development and the yield. As a result, urban trees currently must face on a large range of additional stresses that are less strong or non-existent. This is because climate variabilities and environmental conditions within a city are overall more extreme and harmful to trees and can cause vitality loss and increase mortality risk.

Although many efforts have been made to develop methodologies to assess the drought, it is very difficult to isolate the beginning of a drought, as drought development is slow and very often the drought is not recognized until human activities, or the environment, are affected. Moreover, the effects of a drought can persist over many years after it has ended. In contrast to other extreme events such as floods, which are typically restricted to small regions and well-defined temporal intervals, droughts are difficult to pinpoint in time and space, affecting wide areas over long periods of time. Commonly, there are several climatic drought indices that have been developed to monitor, predict, and assess the severity of drought, such as the Palmer Drought Severity Index (PDSI) (Palmer, 1965), Standardized Precipitation Index (SPI) (McKee et al., 1993), Standardized Precipitation Evapotranspiration Index (SPEI) (Vicente et al., 2010), Vegetation Condition Index (VCI) (Kogan, 1995), Effective Drought Index (EDI) (Byun and Wilhite, 1996), Reconnaissance Drought Index (RDI) (Tsakiris et al., 2007), Soil Moisture Index (SMI) (Nam et al., 2012), Integrated Surface Drought Index (ISDI) (Wu et al., 2013), Multivariate Standardized Drought Index (MSDI) (Hao and AghaKouchak, 2013), and Standardized Vegetation Index (SVI) (Peters et al., 2002) etc. Among these, drought is more severe or less dependent on many factors, including physical, ecological, and human activity. Precipitation is an important factor that should be used to find correlations with these indices. In addition, in order to study the duration of precipitation that affects urban tree, the relationship between precipitation and the index is an important parameter for determining drought areas (Kogan and Guo, 2015). These indices that correlates with physical condition of plants, water content in plants and soil can then indicate drought condition. That is, growth and abundance of vegetation at different weather conditions can be indicated by the Standardized Vegetation Index (SVI) estimations (Peters and Walter-Shea, 2002; Park et al., 2008). The SVI was developed by Peters et al. (2002) that describes the probability of variation from the Normalized Difference Vegetation Index (NDVI) or the Enhanced Vegetation Index (EVI) over multiple times of data. Therefore, the SVI can provide information about the relative vegetation condition compared to the time periods being analyzed. In this study, the SVI was then used as the drought index for monitoring drought impacts on urban trees.

Currently, satellite data can show details from repetition of data recording continually and be able to monitor areas in near real-time with multi-temporal diversity, process of some characteristics change can be monitored better. When satellite data are done with image processing with mathematic equation, they show more outstandingly what to study such as calculating the NDVI which is estimated by determining the ratio of red and near infrared. (Gao et al., 2016; Rimkus et al., 2017). In fact, drought crisis is a spatial problem. Thus, using of satellite data to analyze areas being at risk of drought can increase efficiency in indicating problem conditions. This study focuses on monitoring drought impacts on urban trees that is a challenge to apply and develop a method using remote sensing based on drought monitoring of trees for the management of urban areas. For the urban management, there are many studies to attempt for monitoring and planning urban trees and greenspaces e.g., Brune (2016) in Germany, Vaz Monteiro et al. (2019) in United Kingdom, Intasen et al. (2016) in Bangkok, and Jantakat et al. (2018; 2019; 2020; 2021) in Nakhonratchasima, Thailand. These studies indicated that urban trees and greenspaces can reduce air temperature in the city through plant transpiration, evaporation, shading of surfaces, and reflectance of radiation (Kleerekoper et al., 2012; Doick and Hutchings, 2013). Moreover, mature trees are especially important for shading and interception of precipitation and protecting extreme runoff (Bowler et al., 2010; Gill et al., 2014). Due to the efficiency of satellite data in indicating drought problem, this study uses the tool of Google Earth Engine (GEE) to help for monitoring and evaluating drought impacts on urban trees. The GEE is a web-platform for cloud-based processing of remote sensing data that dedicated to geographic data processing and analysis and can provide massive global geospatial data and many excellent image-processing algorithms, and all the processing is parallel (Gorelick et al., 2017; Kumar and

Mutanga, 2018). These advantages enable researchers to perform large-scale and long-term analysis with minimal cost and equipment (Hansen et al., 2013), including population mapping (Patel et al., 2015), land cover mapping (Huang et al., 2017), cropland mapping (Xiong et al., 2017), surface water mapping (Pekel et al., 2016; Tang et al., 2016), and drought assessment mapping (Sazib et al., 2018).

The main objective of this study is to apply the Google Earth Engine (GEE) for monitoring drought impacts on urban tree with the Standardized Vegetation Index (SVI) in Amphoe Mueang, Nakhonratchasima Province, Thailand. The assessment of SVI is provided for the spatial identification of drought events including duration, intensity, and frequency.

2. Materials and Methods

2.1 Study area

The study area is Amphoe Mueang in Nakhonratchasima province, Thailand (Figure 1) where is a district of Nakhonratchasima province from the total of 32 districts. The study area is in the northeastern region of Thailand and far from Bangkok about 255 km. The total of the study area is 755.6 km^2 that is subdivided into 25 sub-districts (Tambon) as shown in Table 1. The climate is temperate with a daily mean maximum temperature varying from a minimum of 24^oC in December to a maximum of 34^oC in April. The rainfall in Amphoe Muang of Nakhonratchasima province is mainly from the southwest monsoon with the total annual average rainfall of about 193 mm.

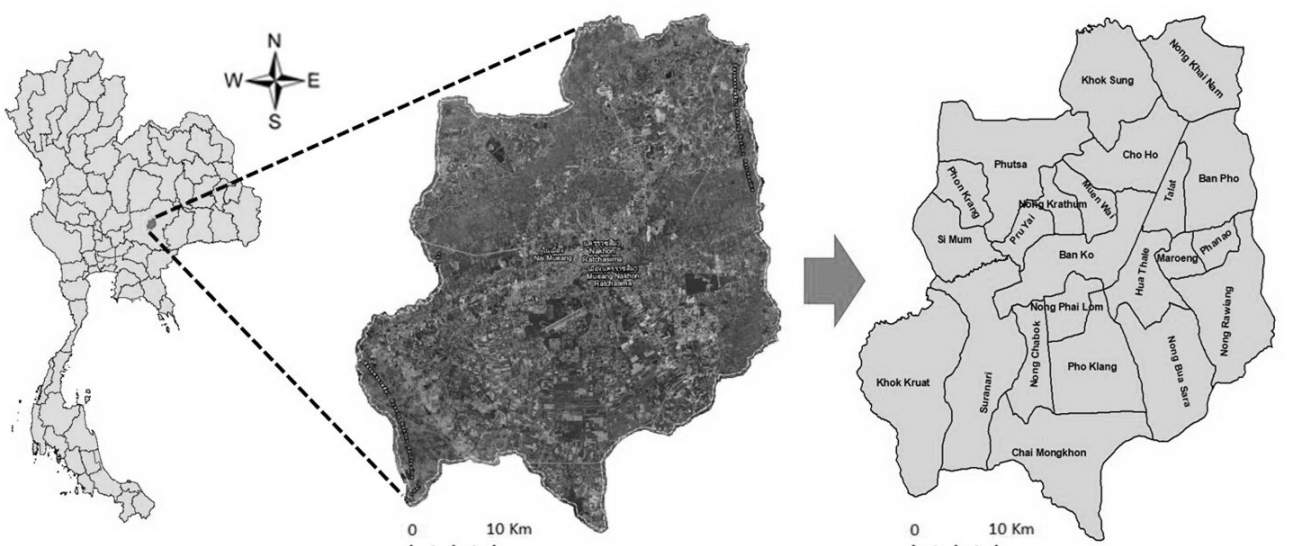

Figure 1. Amphoe Mueang with 25 sub-districts in Nakhonratchasima province, Thailand.

No.	Sub-districts (Tambon)	Population (people)	Area (sq.km.)	Density (people/sq.km.)	Housing (house)
1	Nai Mueang	137,579	37.50	3,668.77	63,302
2	Pho Klang	26,174	55.23	473.9	10,742
3	Nong Chabok	12,168	23.56	516.46	4,991
4	Khok Sung	9,997	30.56	327.12	3,368
5	Maroeng	7,414	10.25	723.31	2,542
6	Nong Rawiang	11,400	54.77	208.14	3,877
7	Pru Yai	9,526	16.63	572.82	4,194
8	Muen Wai	10,296	9.76	1,054.91	4,852
9	Phon Krang	26,174	55.23	473.9	10,742
10	Nong Phai Lom	19,157	17.89	1,070.82	10,305
11	Hua Thale	25,510	15.59	1,636.3	11,255
12	Ban Ko	11,123	11.30	984.33	5,247
13	Ban Mai	17,873	19.55	914.21	6,337
14	Phutsa	9,746	39.36	247.61	2,795
15	Ban Pho	9,045	44.36	203.89	3,293
16	Cho Ho	12,955	26.97	480.34	4,884
17	Khok Kruat	7,059	3.00	2,353	3,387
18	Chai Mongkhon	7,111	60.18	118.16	2,949
19	Nong Bua Sala	19,041	36.61	520.1	10,841
20	Suranari	16,663	49.90	333.92	8,357
21	Si Mum	6,387	15.0	425.8	1,924
22	Talat	6,606	22.20	297.56	2,798
23	Phanao	5,008	18.16	275.77	1,530
24	Nong Krathum	7,648	18.50	413.4	3,575
25	Nong Khai Nam	5,998	43.44	138.07	1,537

Table 1. 25 sub-districts (Tambon) of Amphoe Mueang in Nakhonratchasima province, Thailand (Department of the Interior, 2020).

The population in 2018 was approximately 455,000 people (Department of the Interior, 2020; Thai Meteorological Department, 2021). In terms of topography, the study area is on the Korat plateau, the lower part of northeastern plateau of Thailand. The Lam Takhong river is as a main river flowing through the study area. Currently, Amphoe Mueang Nakhonratchasima is rapidly increasing construction of buildings and roads for business and housing has encroached on surrounding green areas and agricultural land (Wijitkosum and Sriburi, 2008; Chotchaiwong and Wijitkosum, 2019). Moreover, temperatures are rising world-wide due to greenhouse gases trapping more heat in the atmosphere, especially in the urban area. As a results, droughts are becoming longer and more extreme. In Amphoe Mueang Nakhonratchasima, green spaces and urban trees face difficulties in maintenance. Thus, it is necessary to develop an effective tool (e.g., GEE) that can assist in the management of green space and urban tree.

2.2 Methodology

Figure 2 presents the flow chart of the detailed methodology adopted in the study. The methodology was divided into the following main steps including 1) data preparation and pre-processing, 2) SVI calculation, and 3) visualization:

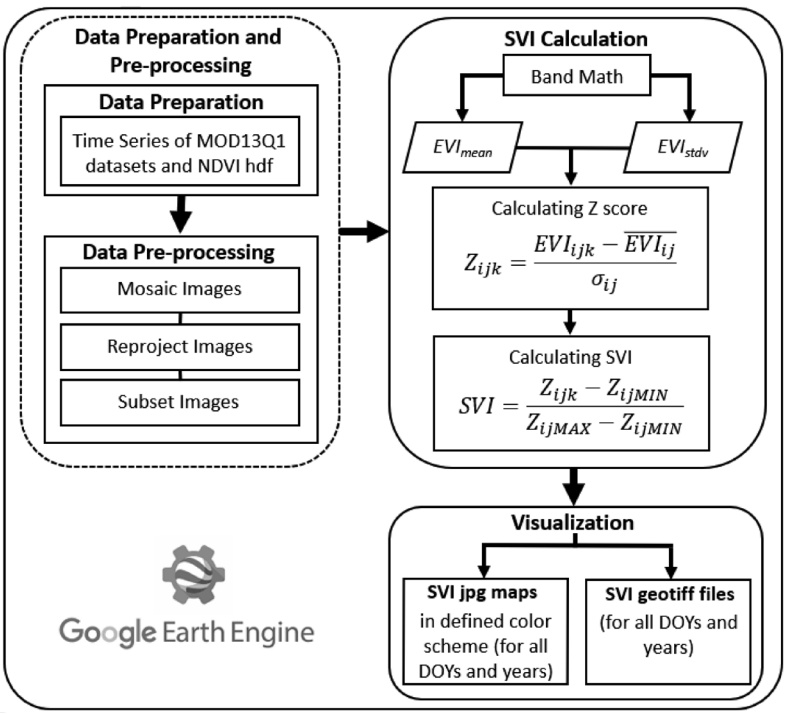

Figure 2. Flow chart of the methodology in the study.

Table 2. Data characteristics of the Terra/MODIS product.

Characteristics	Terra/MODIS product
Acquisition date	Jan. 01, 2000 to May 31, 2021
Serie of product	MOD13Q1
Name of product	Vegetation Indices 16-Day L3 Global 250m
Used data from product	Enhanced Vegetation Index (EVI)
Swath	2,330 km (cross track) by 10 km (along track at nadir)
Spatial resolution	250 m (bands 1-2), 500 m (bands 3-7), 1,000 m (bands 8-36)
Temporal resolution	1-2 Days

2.2.1 Data preparation and pre-processing

Data of the Terra/MODIS satellite from the USGS was used in this study. Generally, the data is designed to track and monitor natural resources, with a swath of about 2,330 km (cross track) by 10 km (along track at nadir), spatial resolution of 250-1,000 m, 36 discrete spectral bands, and collecting data for every point of the earth's surface every 2 days. Two set of MOD13Q1 products, including h27v07 and h28v07, were used for estimating the Enhanced Vegetation Index (EVI) and covered the period since 2000 to recently in this study. The data from the satellite was pre-processed through the radiometric collection and mosaic image processing to combine the two sets of data. The value of the data was then set under the mask to make the cloud area and the water area null and not used in the calculation (Didan et al., 2015). Table 2 shows data characteristics of the Terra/MODIS product.

2.2.2 The calculation of SVI

For calculating the SVI, the study used monthly data from Terra/MODIS of MOD13Q1 series with the EVI format, which can be utilized for monitoring vegetation dynamics. The EVI was based on a standard score (Z-core) deviation from the mean in units of the standard deviation, calculated from the EVI values for each pixel location in each season of 3 seasons in the study area including the hot season (February to May), the rainy season (June to October), and the cold season (November to January). The EVI decouples the soil and atmospheric influences from the vegetation signal by including a feedback term for simultaneous correction. The EVI formula is presented as equation 1 (Didan et al., 2015).

$$EVI = G\frac{NIR - Red}{NIR + C_1 Red - C_2 Blue + L} \quad \text{(e.q.1)}$$

where *NIR*, *Red*, and *Blue* are the full or partially atmospheric-corrected surface reflectances, *L* is the canopy background adjustment for correcting the nonlinear, differential NIR and red radiant transfer through a canopy, C_1 and C_2 are the coefficients of the aerosol resistance term, and *G* is a gain or scaling factor. The coefficients adopted for the MODIS/EVI algorithm are, *L*=1, C_1=6, C_2=7.5, and *G*=2.5 (Didan et al., 2015).

The Z-core can be calculated via the following equation 2 (Peters et al., 2002; Anyamba and Tucker, 2012).

$$Z_{ijk} = \frac{EVI_{ijk} - \overline{EVI_{ij}}}{\sigma_{ij}} \quad \text{(e.q.2)}$$

where Z_{ijk} is the z-value for the pixel *i* during week *j* for year *k*, EVI_{ijk} is the weekly EVI value for pixel *i* during week *j* for year *k*, $\overline{EVI_{ij}}$ is the mean EVI for pixel *i* during week *j* over n years, and σ_{ij} is the standard deviation of pixel *i* during week j over n years.

Basically, the Z-score value from e.q.1 indicates how many standard deviations an element is away from the mean and how spread out the set of data is. A low standard deviation implies that the data is closely clustered around the mean whereas a high standard deviation implies that the data is dispersed over a wider range of values (Columbia Business School and Columbia University, 2003; Trek, 2018). Therefore, the Z-score value is consistent with a standard normal distribution with the mean of 0 and standard deviation of 1 to examine hypothesis from pixel locations in each season of the years 2016, 2017, 2018, 2019 and 2020. The probability value of the SVI of the standard score of EVI to reflect the probability of plant conditions. The SVI can be calculated from equation 3 (Peters et al., 2002).

$$SVI = \frac{(Z_{ijk} - Z_{ijMIN})}{Z_{ijMAX} - Z_{ijMIN}} \quad \text{(e.q.3)}$$

where Z_{ijk} is the z-value for the pixel i during week j for year *k*, Z_{ijMIN} is the minimum of z-value for pixel *i* during week *j*, and Z_{ijMAX} is the maximum of z-value for pixel *i* during week *j*.

Based on the equation 2, the probability of each pixel was expressed as the SVI, to present the greenness of the vegetation in terms of the probability of each pixel during different seasons of different periods. In this study, the long-term period of 20 years (2000-2021) was conducted and compared the high-level drought and low-level drought during such a period by seasons. The range of the SVI value of more than zero but less than one (0<SVI<1) described that 0 was the lowest standard deviation of the EVI at the pixel in that period over a period of 20 years and 1 was the highest standard deviation of the EVI at the pixel in that period over a period of 20 years.

For the spatial analysis of drought intensity in this study, it was classified by critical levels of vegetation in each month of the years 2016, 2017, 2018, 2019 and 2020. The drought levels of the SVI were classified into 5 levels based on SVI values of the standard deviation including very low drought or very high vegetation (1.50 to 2.50), low drought or high vegetation (0.50 to 1.50), moderate drought or moderate vegetation (-0.50 to 0.50), high drought or low vegetation (-1.50 to -0.50), and very high drought or very low vegetation (-2.50 to -1.50) as presented in Table 3.

2.2.3 The visualization in Google Earth Engine

In this study, Google Earth Engine (GEE) (more information on the website: https://developers.google.com/earth-engine/guides/playground) was used for the analysis and visualization of drought levels. One major advantage of GEE is the accessibility of global time series data which are already loaded on Google's servers and contained a certain type or quality of data. The GEE code can be found in the recommended practice of the United Nations Office for Outer Space Affairs (2020). After the calculations, the GEE can display the latest SVI image in the map section, the latest EVI image, and the mean EVI image of the whole timescale in the layers. The GEE can also show the charts of the EVI and SVI overtime by taking the mean of all pixels in the study area for each season. Moreover, the results of the SVI jpg and geotiff files were provided for downloading from the GEE.

3. Results and Discussion

3.1 Spatial Drought monitoring through the SVI

The SVI was used as the drought index since 2000 to recently for more than 20 years to access drought impacts on urban tree in this study. For analyzing the spatial drought monitoring with the SVI, the study used satellite data from 2016 to 2020 for examining hypothesis from pixel locations in each season of the years 2016, 2017, 2018, 2019 and 2020. In this study area, there are 3 seasons including cold season (November to January), summer season (February to May), and rainy season (June to October). Thus, this study estimated the mean monthly SVI for each season with the SVI values from -2.5 (high

Table 3. The classification of SVI and drought levels.

Level	SVI value	SVI category	Drought category
1	1.50 to 2.50	Very high vegetation	Very low drought
2	0.50 to 1.50	High vegetation	Low drought
3	-0.50 to 0.50	Moderate vegetation	Moderate drought
4	-1.50 to -0.50	Low vegetation	High drought
5	-2.50 to -1.50	Very low vegetation	Very high drought

drought) to 2.5 (low drought). The results show that the SVI values (-2.50 to -1.50) in the condition of very high drought were found mostly in 2019, especially in summer season. In addition, there is an increasing trend of higher drought in the middle of the study area (Tambon Nai Mueang) and in the south part of the study area (Tambon Nong Chabok, Pho Klang, and Nong Bua Sala) as shown in Table 4.

Table 4. Analyzing the spatial drought monitoring with the SVI in each season in Amphoe Mueang of Nakhonratchasima province, Thailand.

Year	November to January	February to May	June to October
	Cold Season	Summer Season	Rainy Season
2020	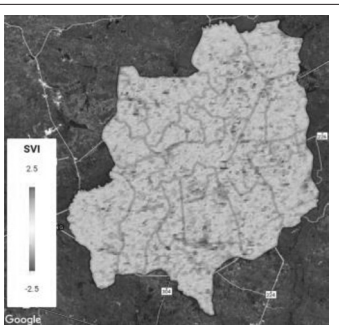	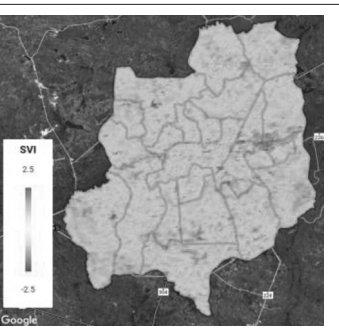	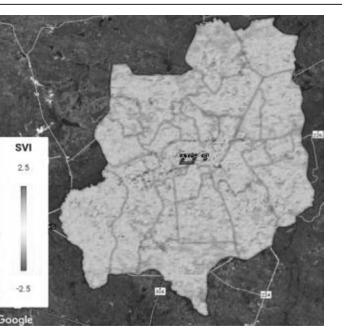
2019	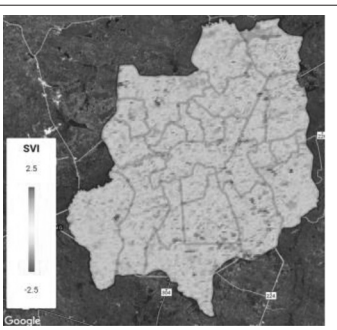	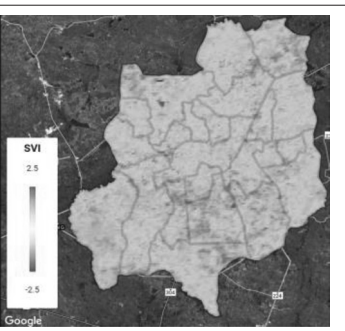	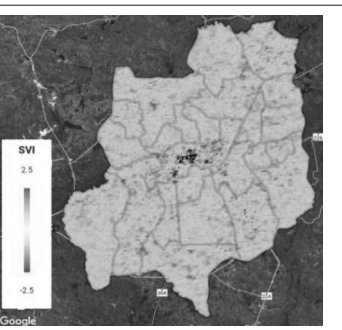
2018	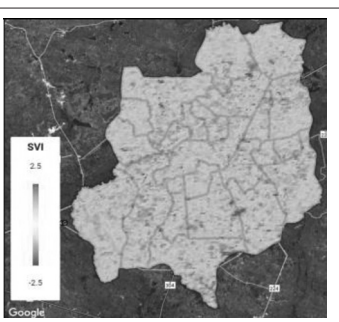	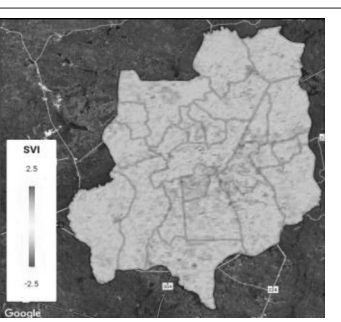	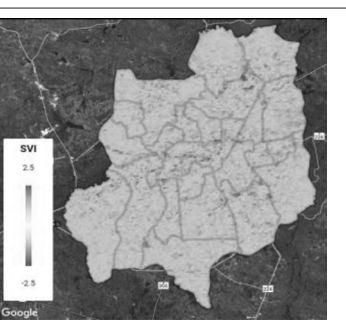

Table 4. Analyzing the spatial drought monitoring with the SVI in each season in Amphoe Mueang of Nakhonratchasima province, Thailand. (Continue)

Year	November to January	February to May	June to October
	Cold Season	Summer Season	Rainy Season
2017	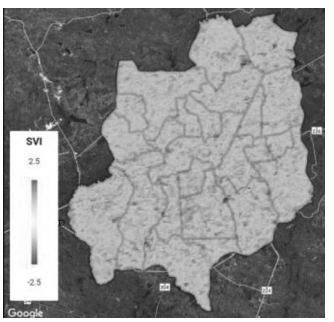	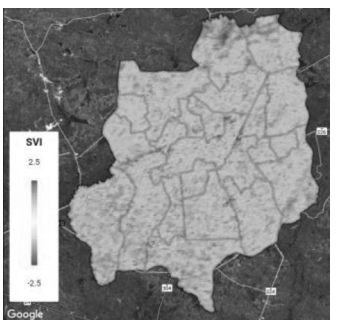	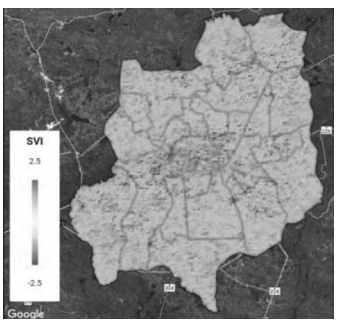
2016		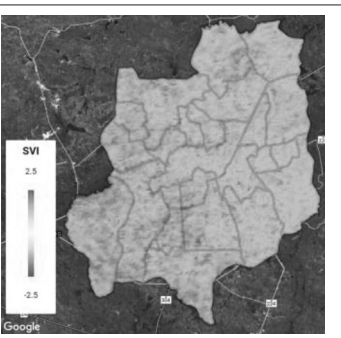	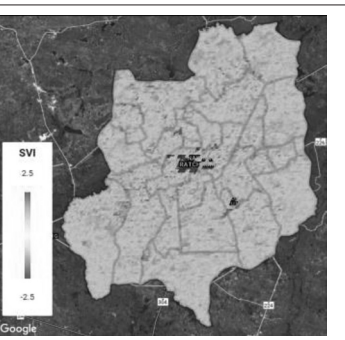

3.2 Timeseries of Drought monitoring with the SVI and EVI

Data satellite from year 2000 to recently were collected and calculated for the mean of SVI and EVI values in the study area. Figure 3 and 4 presented the timeseries of the mean of SVI and EVI, respectively. Based on the SVI timeseries, the condition of high drought (-1.5 to -0.5) was obviously found in years of 2002, 2005, 2015, 2016, and 2019 in accordance with the mean of EVI timeseries in Figure 4.

3.3 Drought monitoring through Google Earth Engine

Figure 5 and 6 present the results of drought monitoring in the study area through Google Earth Engine (GEE) app. The GEE can display the SVI, EVI, and mean EVI image of the whole timescale in the map section and can receive a pixel value from the visualized images by clicking on a location within the study area. The charts, which display the EVI and SVI values over time by taking the mean of all pixels in the study area for each acquisition date. Briefly, a positive SVI indicates a good vegetation condition and a negative SVI indicates a worse vegetation condition. The GEE script can be found and used in the available website of https://code.earthengine.google.com/ and https://juntakut37.users.earthengine.app/view/drought-monitoring-in-amphoe-mueang-nakhonratchasima-province. For assessing of accuracy of the study results, according to field surveying based on the research project of geospatial technology along street trees in Nakhonratchasima City Municipality (https://www.gis-streettreets.ibuddyweb.com) and Google View Street, urban trees during 2014 to 2020 in the study area were shown to compare with the SVI results in Table 5.

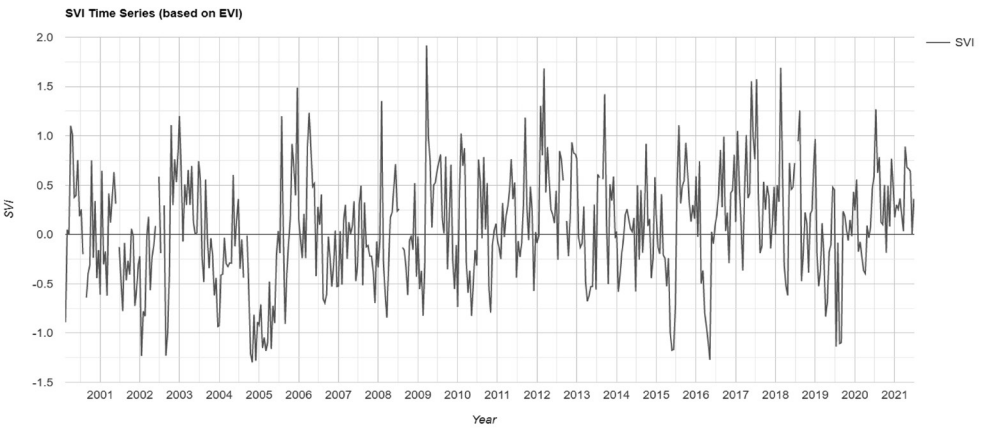

Figure 3. Timeseries of drought monitoring with the mean of SVI in the study area.

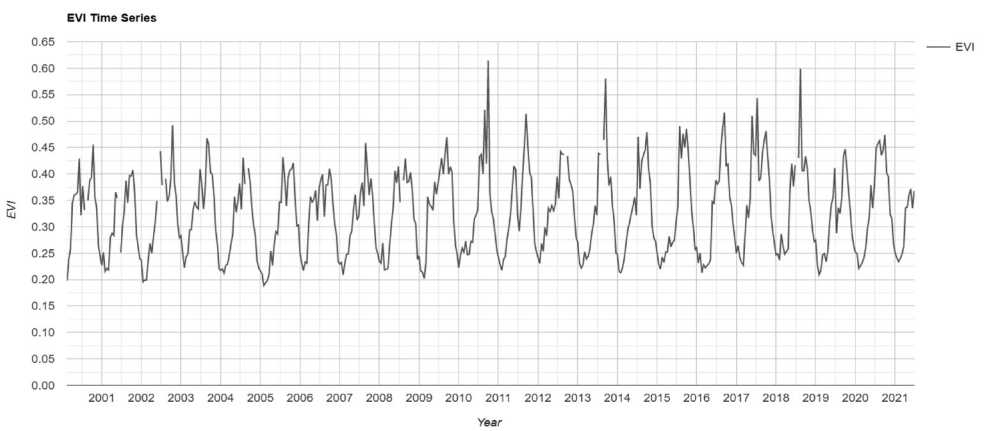

Figure 4. Timeseries of the mean of EVI in the study area.

4. Conclusions

In this study, the GEE was applied to monitor drought impacts on urban tree with theSVIinAmphoeMueang,Nakhonratchasima Province, Thailand. The data of Terra/ MODIS satellite from 2000 to recently was analyzed and accessed drought impacts on urban tree in the study area. For analyzing the spatial drought monitoring with the SVI, the study used satellite data from 2016 to 2020 for examining hypothesis from pixel locations in each season of the years 2016, 2017, 2018, 2019 and 2020. The results of the study indicated that the SVI values (-2.50 to -1.50) in the condition of very high drought were found mostly in 2016 and 2019, especially in summer season and with an increasing trend of higher drought in the middle of the study area (Tambon Nai Mueang) and in the south part of the study area (Tambon Nong Chabok, Pho Klang, and Nong Bua Sala), probably due to the less precipitation rate in 2016 and 2019. Based on the SVI timeseries, the condition of high drought (-1.5 to -0.5) was obviously found in years of 2002, 2005, 2015, 2016, and 2019 in accordance with the mean of EVI timeseries, especially in the beginning of summer season. As a result, urban trees should be carefully maintained during and after the summer season to aid in the recovery of trees in the study area, such as by watering and fertilizing them on a regular

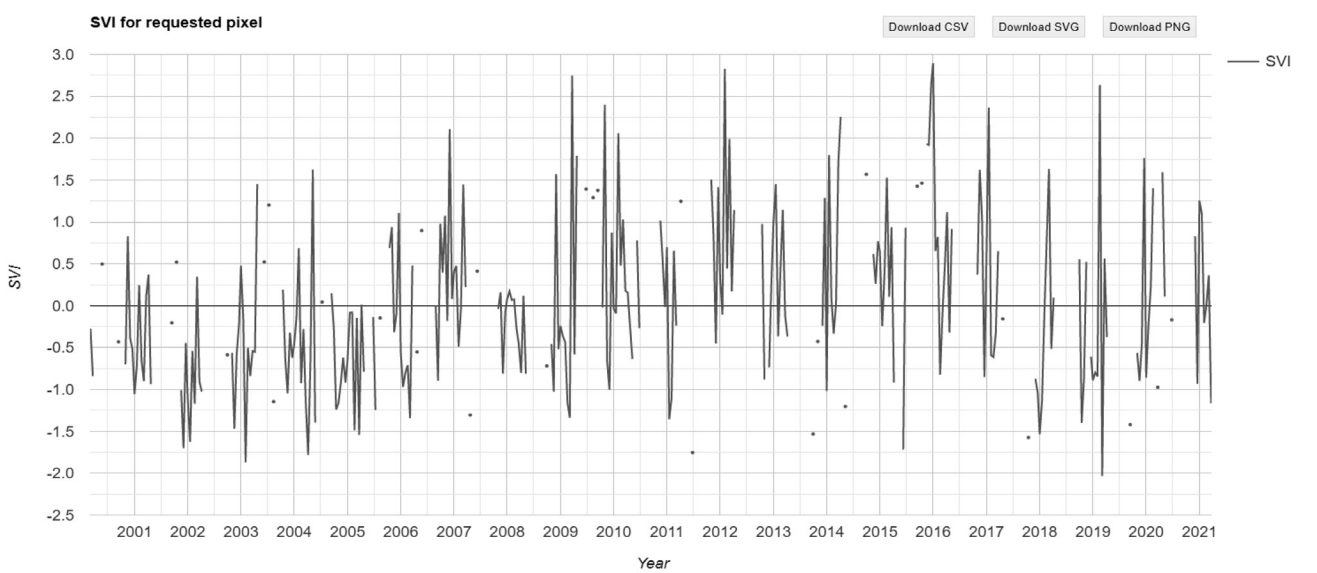

Figure 5. Displaying the SVI image and timescale from requested pixel (Jomsurangyard Rd.).

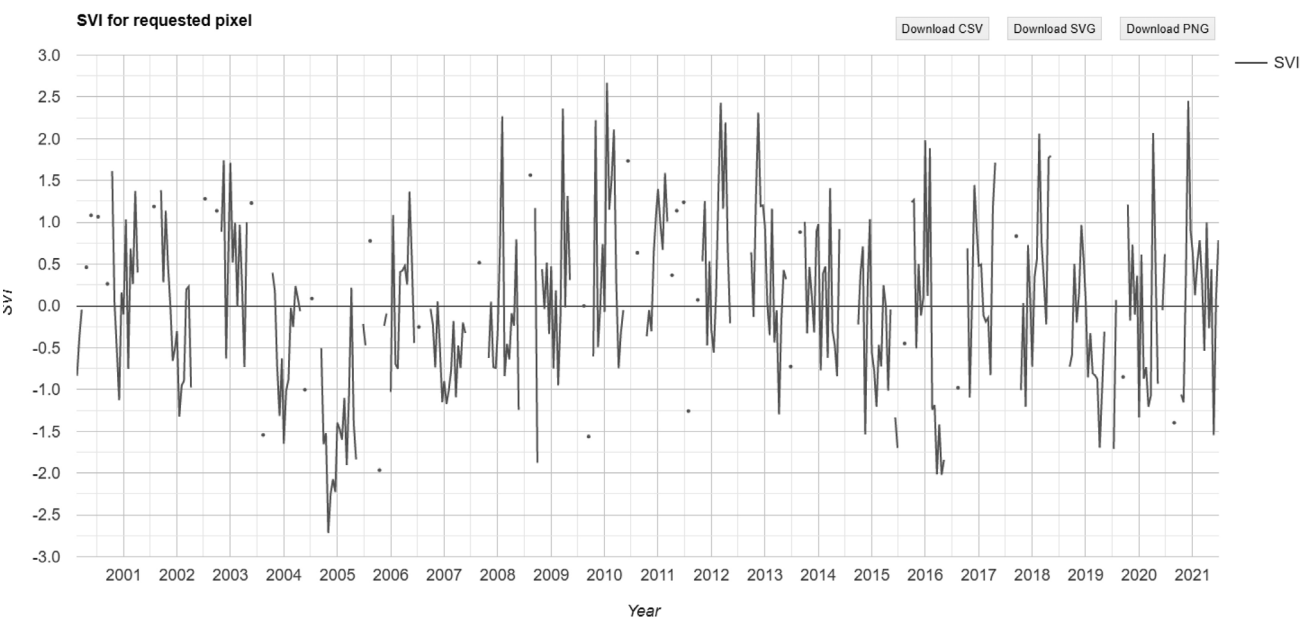

Figure 6. Displaying the SVI image and timescale from requested pixel (Sueb Siri Rd.)

Table 5. Urban tree conditions during 2014 to 2020 on Jomsurangyard Rd. and Sueb Siri Rd. in the study area.

Jomsurangyard Rd. (Tambon Nai Mueang, Amphoe Mueang, Nakhonratchasima Province)			Sueb Siri Rd. (Tambon Nong Chabok, Amphoe Mueang, Nakhonratchasima Province)		
Year	Month	Urban Trees	Year	Month	Urban Trees
2014	March (SVI = -1.2) High drought		2014	February (SVI = -0.7) High drought	
2017	April (SVI = +0.7) Low drought		2018	September (SVI = +0.7) Low drought	
2018	September (SVI = +0.5) Low drought		2018	October (SVI = +1.0) Low drought	
2020	September (SVI = +0.2) Moderate drought		2020	September (SVI = +2.2) Very low drought	

basis. After years of severe drought, it is likely that new trees should be planted. According to the study, the GEE can display the SVI, EVI, and mean EVI image of the whole timescale in the study area, which can help keep urban trees healthy and less vulnerable to drought stress. Conclusively, the application of the GEE for monitoring drought impacts on urban tree with the SVI can be an efficiency tool for urban planning and taking care urban tree health in near real-time period. For further research, the study will use data from the results of this study to run a model and predict a future drought trending in the study area.

References

Anyamba, A., & Tucker, C. J. (2012). Historical perspective of AVHRR NDVI and vegetation drought monitoring. *Remote Sens Drought: Innovative Monit Approaches, 23*.

Bowler, D.E., Buyung-Ali, L., Knight, T. M., & Pullin, A.S. (2010). Urban greening to cool towns and cities: A systematic review of the empirical evidence. *Landscape and Urban Planning, 97*(3), 147–155.

Brune, M. (2016). Urban trees under climate change. Potential impacts of dry spells and heat waves in three German regions in the 2050s. *Report 24. Climate Service Center Germany*, Hamburg.

Byun, H. R., & Wilhite, D. A. (1996). Daily quantification of drought severity and duration. J. *Clim.; 5*, 1181–1201.

Chen, T., van der Werf, G. R., de Jeu, R. A. M., Wang, G., & Dolman, A. J. (2013). A global analysis of the impact of drought on net primary productivity. *Hydrol. Earth Syst. Sci.17*: 3885–3894.

Chotchaiwong, P., & Wijitkosum, S. (2019). Relationship between land surface temperature and land use in Nakhon Ratchasima City, Thailand. *Engineering Journal; Vol.23*(4): 1-14.

Columbia Business School and Columbia University. (2003). *Statistical Sampling and Regression: t-Distribution*. Retrieved from: http://ci.columbia.edu/ci/premba_test/c0331/s7/s7_4.html.

Department of the Interior. (2020). Statistics, population, and house statistics for the year 2019.

Didan, K., Munoz, A. B., Solano, R., & Huete, A. (2015). *MODIS Vegetation Index User's Guide. Vegetation Index and Phenology Lab. The University of Arizona.* Retrieved from https://lpdaac.usgs.gov/documents/103/MOD13_User_Guide_V6.pdf

Doick, K., & Hutchings, T. (2013). Air temperature regulation by urban trees and green infrastructure, *Farnham: Forestry Commission (UK)*. 1-10 pages. Available at: http://www.forestry.gov.uk/PDF/FCRN012.pdf/$FILE/FCRN012.pdf [Accessed January 8, 2015].

Gao, Y., Markkanen, T., Thum, T., Aurela, M., Lohila, A., Mammarella, I., Kämäräinen, M., Hagemann, S., & Aalto, T. (2016). Assessing various drought indicators in representing summer drought in boreal forests in Finland. *Hydrology and Earth System Sciences; 20*, 175–191.

Gill, S. E., Handley, J. F., Ennos, A. R., & Pauleit, S. (2014). Adapting The Role Cities for Climate of the Green Change: Infrastructure. *Built Environment, 33*(1), 115–133.

Gorelick, N., Hancher, M., Dixon, M., Ilyushchenko, S., Thau, D., & Moore, R. (2017). Google Earth Engine: Planetary-scale geospatial analysis for everyone. Remote Sens. *Environ.; Vol. 202*, 18–27.

Hansen, M. C., Patel, N. N., Joshi, A. R., Huang, H., & Xiong, J. (2013). High-resolution global maps of 21st-century forest cover change. *Science; Vol. 850*: 2011–2014.

Hao, Z. C., & AghaKouchak, A. (2013). Multivariate Standardized Drought Index: A parametric multi-index model. Adv. *Water Resour.; 57*, 12–18.

Huang, H., Chen, Y., Clinton, N., Wang, J., Wang, X., Liu, C., Gong, P., Yang, J., Bai, Y., Zheng, Y., & Zhu, Z. (2017). Mapping major land cover dynamics in Beijing using all landsat images in Google Earth Engine. Remote Sens. *Environ.; Vol.202*: 166–176.

Intasen, M., Hauer, R. J., Werner, L. P., & Larsen, E. (2016). Urban forest assessment in Bangkok, Thailand. *Journal of Sustainable Forestry; Vol. 36*(2).

Jantakat, Y., Juntakut, P., & Kranka, S. (2018). Applied Geo-Informatics Technology to Urban Green Space Management on Role of Stormwater Runoff Reducing and Increasing of Subsurface Water. *2nd Conference on Geoinformatics,* Feb. 1-2 in Bangkok, Thailand; 15-24.

Jantakat, Y., Juntakut, P., Plaiklang, S., Arree, W., & Jantakat, C. (2019). Spatiotemporal Change of Urban Agriculture using Google Earth Imagery: A Case of Municipality of Nakhonratchasima City, Thailand. *The International Archives of the Photogrammetry, Remote Sensing and Spatial Information Sciences*, Vol. XLII-2/W13. ISPRS Geospatial Week 2019, 10-14 June, Enschede, The Netherlands; 1301-1306.

Jantakat, Y., Juntakut, P., Kisanthia, P., & Udom, K. (2020). Application of Geographic Information System via Web for Class of Local Resource and Environmental Management. *The Journal of Spatial Innovation Development; Vol. 1*(2): 70-82.

Jantakat, Y., Hudkhuntod, T., Muankhamla, A., Mangkalanan, S., Garcia, L. E., Srithumma, K., Rengprapan, S., & Juntakut, P. (2021). ArcGIS Web-based Rapid Application Development for Presenting Urban Street Trees on Sidewalks. International Journal of Building, Urban, *Interior and Landscape Technology (BUILT), 17,* 29-40. Retrieved from https://ph02.tci-thaijo.org/index.php/BUILT/article/view/244005

Kleerekoper, L., van Esch, M., & Salcedo, T. B. (2012). How to make a city climate-proof, addressing the urban heat island effect. *Resources, Conservation and Recycling, 64*, 30-38.

Kogan, F. N. (1995). Droughts of the late 1980s in the United States as derived from NOAA polar-orbiting satellite data. Am. *Meteorol; 76*: 655–668.

Kogan, F., & Guo, W. (2015). Agricultural Drought Detection and Monitoring Using Vegetation Health Methods. In Remote Sensing of Water Resources, Disasters, and Urban Studies; THENKABAIL P.S., Ed.; *CRC Press: Boca Raton*, FL, USA: 339.

Kumar, L., & Mutanga, O. (2018). Google Earth Engine applications since inception: Usage, trends, and potential. *Remote Sens.; Vol. 10*(10).

McKee, T. B., Doesken, N. J., & Kleist, J. (1993). The relationship of drought frequency and duration to time scales. In *Proceedings of the Eighth Conference on Applied Climatology*, Boston, MA, USA, 17–22 Jan.: 179–184.

Nam, W. H., Choi, J. Y., Yoo, S. H., & Jang, M. W. (2012). A decision support system for agricultural drought management using risk assessment. *Paddy Water Environ.; 10*, 197–207.

Palmer, W.C. (1965). Meteorological Drought. White R.M., Ed.; U.S. Weather Bureau: Washington, DC, USA.

Park, J. S., Kim, K. T., & Choi, Y. S. (2008). Application of Vegetation Condition Index and Standardized Vegetation Index for Assessment of Spring Drought in South Korea, in *IGARSS 2008-2008 IEEE International Geoscience and Remote Sensing Symposium, 3*: 774.

Patel, N. N., Angiuli, E., Gamba, P., Gaughan, A., Lisini, G., Stevens, F. R., Tatem, A. J., & Trianni, G. (2015). Multitemporal settlement and population mapping from Landsat using Google Earth Engine. Int. J. Appl. Earth Observ. *Geoinf.; Vol.35*: 199–208.

Pekel, J. F., Cottam, A., Gorelick, N., & Belward, A. S. (2016). High-resolution mapping of global surface water and its long-term changes. *Nature; Vol.540*(7633): 418–422.

Peters, J. A., Walter-Shea, E. A., Ji, L., Andres, V., Michael, H., & Svoboda, M. D. (2002). Drought Monitoring with NDVI-Based Standardized Vegetation Index. *Photogrammetric Engineering & Remote Sensing, 68*(1): 71.

Rimkus, E., Stonevicius, E., Kilpys, J., Maciulyte, V., & Valiukas, D. (2017). Drought identification in the eastern Baltic region using NDVI. *Earth System Dynamics; 8*, 627–637.

Sazib, N., Mladenova, L., & Bolten, J. (2018). Leveraging the Google Earth Engine for Drought Assessment Using Global Soil Moisture Data. Remote Sens; 10(8), 1265.

Thai Meteorological Department. (2021). *Climatological Center*. Retrieved from http://climate.tmd.go.th/map/thailand

Trek, S. (2018). Statistics and probability. Retrieved from: https://stattrek.com/

Tsakiris, G., Pangalou, D., & Vangelis, H. (2007). Regional drought assessment based on the Reconnaissance Drought Index (RDI). Water Resour. *Manag.; 21*, 821–833.

United Nations Office for Outer Space Affairs. (2020). *Knowledge Portal*. Retrieved from https://www.un-spider.org/advisory-support/recommended-practices/recommended-practice-drought-monitoring-using-standard

Vaz Monteiro, M., Handley, P., Morison, J. I. L., & Doick, K. J. (2019). The role of urban trees and greenspaces in reducing urban air temperatures. *Forest Research*. ISBN: 978-0-85538-984-0.

Vicente, S. S. M., Begueria, S., & Lopez-Moreno, J. I. (2010). A multiscalar drought index sensitive to global warming: The Standardized Precipitation Evapotranspiration Index. *J. Clim*; 23: 1696–1718.

Wang, J. J., & Meng, Y. B. (2013). An analysis of the drought in Yunnan, China, from a perspective of society drought severity. *Nat. Hazards, 67*: 431–458.

Wang, Q. F., Wu, J. J., Lei, T. J., He, B., Wu, Z. T., Liu, M., Mo, X. Y., Geng, G. P., Li, X. H., & Zhou, H. K. (2014). Temporal-spatial characteristics of severe drought events and their impact on agriculture on a global scale. *Quat. Int. 349*: 10–21.

Wijitkosum, S., & Sriburi, T. (2008). Impact of urban expansion on water demand: The case study of Nakhon Ratchasima city, Lam Ta Kong Watershed. *Nakhara: Journal of Environmental Design and Planning; Vol.4*: 69-88.

Wu, J. J., Zhou, L., Liu, M., Zhang, J., Leng, S., & Diao, C. Y. (2013). Establishing and assessing the Integrated Surface Drought Index (ISDI) for agricultural drought monitoring in mid-eastern China. *Int. J. Appl. Earth Obs.; 23,* 397-410.

Xiong, J., Thenkabail, S., Gumma, M. K., Teluguntla, P., Poehnelt, J., Congalton, R. G., Yadav, K., & Thau, D. (2017). Automated cropland mapping of continental Africa using Google Earth Engine cloud computing. ISPRS J. Photogramm. *Remote Sens.; Vol.126*: 225–244.

Zhang, Z. X., Chen, X., Xu, C. Y., Hong, Y., Hardy, J., & Sun, Z. H. (2015). Examining the influence of river-lake interaction on the drought and water resources in the Poyang Lake basin. *J. Hydrol. 522*: 510–521.